Z. Rueger and R. S. Lakes *
University of Wisconsin-Madison
Department of Engineering Physics
1500 Engineering Drive
Madison, WI 53706, USA
zdrueger33@gmail.com
* Corresponding author rlakes@wisc.edu

March 10, 2020

Abstract

A dense closed cell foam is studied to determine which continuum theory of elasticity is applicable. Size effects inconsistent with classical elasticity are observed. The material exhibits a characteristic length scale considerably larger, by more than a factor 6, than the largest observable structure size. The Cosserat coupling number N is shown to be small, via measurements of size effects in square section bars, comparison with size effects in round section bars, and determination of warp of a square section bar in torsion. For this material, the couple stress theory is excluded and the modified couple stress theory is excluded. Theories that force constants to their thermodynamic limits do not apply to this foam. The role of other generalized continuum theories is considered.

Keywords Elasticity - Cosserat - micropolar - generalized continuum

1   Introduction

In classical elasticity there is no length scale in the theory. Any length scale associated with microstructure in the material under study is therefore neglected. If the microstructure is sufficiently small compared with the length scale of the experiment, classical elasticity is entirely adequate. When the nature and size of the microstructure cannot be neglected, generalized continuum theories may be considered. Cosserat elasticity is a generalized continuum theory that allows rotation of points as well as translation; couple stress as well as stress [1, 2, 3]. It is not the only generalized continuum theory but from the perspective of experiment it is expedient to use it because analytical solutions for interpretation of experiments are available [4] [5] [6] [7] [8].

The constitutive equations for linear isotropic Cosserat elasticity [3] are:

$$\sigma_{ij} = 2G\epsilon_{ij} + \lambda\epsilon_{kk}\delta_{ij} + \kappa e_{ijk}(r_k - \phi_k) \tag{1}$$

$$m_{ij} = \alpha\phi_{k,k}\delta_{ij} + \beta\phi_{i,j} + \gamma\phi_{j,i} \tag{2}$$

The stress σ_{ij} can be asymmetric in a Cosserat solid. The moment from the asymmetric stress is balanced by a couple stress, m_{ij}. Gradients in the rotation ϕ_i of points give rise to distributed moments. The macro-rotation $r_k = \frac{1}{2}e_{klm}u_{m,l}$ based on the antisymmetric part of gradient of displacement u_i need not equal the rotation of points; e_{jkm} is the permutation symbol.

There are six independent elastic constants for an isotropic Cosserat solid. Constants λ, G have the same meaning as in classical elasticity. Constants α, β, γ provide sensitivity to rotation gradients and κ

quantifies the coupling between macro and micro rotation fields. Technical constants, derived from these elastic constants are beneficial for physical insight. The technical elastic constants are: Young's modulus E, shear modulus G, Poisson's ratio ν, characteristic length, torsion ℓ_t, characteristic length, bending ℓ_b, coupling number N, polar ratio Ψ:

$$E = \frac{2G(3\lambda + 2G)}{2\lambda + 2G} \tag{3}$$

$$G \tag{4}$$

$$\nu = \frac{\lambda}{2(\lambda + G)} \tag{5}$$

$$\ell = \sqrt{\frac{\beta + \gamma}{2G}} \tag{6}$$

$$\ell_b = \sqrt{\frac{\gamma}{4G}} \tag{7}$$

$$N = \sqrt{\frac{\kappa}{2G + \kappa}} \tag{8}$$

$$\Psi = \frac{\beta + \gamma}{\alpha + \beta + \gamma} \tag{9}$$

The physical meaning of the classical constants E, G, ν is well known. In a Cosserat solid these are the constants measured in the absence of gradients in deformation. The characteristic lengths ℓ_t and ℓ_b are based on ratios of rotation gradient sensitivity to classical elastic constants. They represent the length scale at which deviations from classical elasticity become notable. They need not correspond to structural length scales in the material. Experiment and homogenization studies reveal the characteristic length may be zero, smaller than the structure size, or larger than the structure size. The coupling number N is a dimensionless measure of the coupling between the rotation field and the displacement field. The range based on energy considerations is from zero to 1. Nonclassical effects are larger in magnitude for large N than for small N. The polar ratio Ψ is analogous to Poisson's ratio in classical solids.

Some particular cases are known. If one assumes for simplicity, after Koiter [9], that the macrorotation and microrotation vectors are equal, then in Cosserat elasticity, $N = 1$, or equivalently $\kappa \to \infty$. This case is called couple stress elasticity which has four elastic constants; the nonclassical ones correspond to ℓ_t and ℓ_b in the Cosserat case. Some more recent authors, e.g. [10], have reintroduced variants of couple stress theory. In one such version [11], there is only one nonclassical constant, a characteristic length which we call ℓ_y to distinguish it from other lengths.

Various authors define the characteristic length differently. For example a bending Cosserat characteristic length is defined [4] as $\ell_g = \sqrt{(1 - \nu^2)\frac{\gamma}{E}}$ or is defined [5] as $\ell_k = \sqrt{\frac{\gamma(2G + \kappa)}{4G\kappa}} = \ell_b/N$. In couple stress elasticity [9] the characteristic length for bending is called ℓ; size effects in torsion are expressed in terms of ℓ and a ratio η.

To interpret the couple stress length ℓ_y consider a plate bending example in Cosserat elasticity [4]. The bending rigidity ratio for a plate of full thickness h, is $\Omega = [1 + 24(1 - \nu)(\ell_b/h)^2]$. The rigidity ratio is the ratio of structural rigidity observed for a given thickness to the rigidity for asymptotically large thickness in which strain gradients tend to zero. For modified couple stress theory, the plate bending rigidity ratio is $\Omega = [1 + 6(1 - \nu)(\ell_y/h)^2]$. So $\ell_y = 2\ell_b$, which corresponds to assuming in a Cosserat solid that $\beta/\gamma = 1$. Also, the rigidity ratio for torsion of a Cosserat elastic circular rod of radius r, $\Omega = 1 + 6(\ell_t/r)^2$ for $N = 1$. An expression identical to the Cosserat $N = 1$ case was given for modified couple stress elasticity [11] in which $\ell_y = \ell_t$. A similar expression in terms of a bending length and a dimensionless ratio is given for couple stress elasticity [9].

So, modified couple stress theory entails $\frac{\beta}{\gamma} = 1$ and $N = 1$. Couple stress theory entails $N = 1$ but allows a range of ratio of characteristic length in bending to that in torsion.

As for the asymptotic rise in the Cosserat rigidity for small width it has been suggested [12] that one choose limiting values of some Cosserat constants to prevent divergence of the structural rigidity for small specimen width. For example $\Psi = 1.5$ (its upper bound) gives rise to a finite intercept on the ordinate of

a plot of normalized structural rigidity vs. size for torsion and $\frac{\beta}{\gamma} = \pm 1$ (the upper or lower bound) gives rise to a finite intercept on the ordinate for bending. This corresponds to a restricted version of Cosserat elasticity which differs from the restriction of couple stress elasticity, which entails divergence of the rigidity for small width.

If the solid has no more freedom than that of a Cosserat solid, and possibly less, then it is straightforward to determine by experiment which theory applies. The values of characteristic lengths ℓ_t and ℓ_b are determined by size effect experiments in torsion and bending respectively. If there are no measurable size effects, the material may be described as classical. If nonzero characteristic lengths are inferred from experiment, the ratio of these lengths gives $\frac{\beta}{\gamma}$ via

$$\frac{\ell_t^2}{\ell_b^2} = 2(\frac{\beta}{\gamma} + 1) \tag{10}$$

One can also extract $\frac{\beta}{\gamma}$ from the sigmoid curvature of the lateral surfaces in bending of a square cross section bar [6]. The value of N may be determined from the shape of the size effect curve for small specimens.

Cosserat elastic effects have been studied in a variety of materials. A composite with spherical inclusions was found to have a characteristic length of zero and to be classical [4]. Cosserat effects have been observed in bone, foams [13] [14] [15] and lattices [16]. Characteristic lengths were comparable to the structure size. A non-cohesive granular assembly of metal spheres was studied via waves [17]. A value of κ was inferred but characteristic lengths were not obtained. Homogenization analysis of chiral honeycombs revealed a Cosserat characteristic length comparable to the cell size [18]. Planar bars with an array of circular holes exhibited size effects [19]; a Cosserat characteristic length in bending was found to be on the order of the hole spacing.

A dense polyurethane foam [13] was studied for Cosserat effects via size effect measurements on round specimens. Elastic constants were found to be $E = 300$ MPa, $G = 104$ MPa, $\nu = 0.44$, $\ell_t = 0.62$ mm, $\ell_b = 0.327$ mm, $N = 0.2$, $\Psi = 1.5$. The density was 340 kg/m^3; the foam was closed cell with cells of diameter from 0.05 to 0.15 mm. Results and curve fits were plotted in the form rigidity divided by diameter squared vs. diameter squared because the tangent of such a plot gives an intercept on the abscissa which corresponds to the characteristic length.

In the present research, this dense foam was studied further in square section specimens with the aim of exploring the consequences of weak coupling. To that end, specimens of square cross section are examined via size effects and study of warp deformation.

2 Methods

2.1 Materials

The material under study is high-density rigid polyurethane closed-cell foam. The material, called last-a-foam, is commercially available [20]; it is used for composite panel cores, flotation devices and other uses. The variant used, FR3720, with nominal density 20 pounds per cubic foot, was chosen because the mechanical properties were stated to be isotropic at this density based on manufacturer specifications. The material as received was a block 22.2 mm by 190 mm by 178 mm. The density of specimens for the square section size effect study was 361 kg/m^3. Typical microstructure is shown in Figure 1. On visual examination the heterogeneity is not obvious. The largest cells, about 0.15 mm in diameter, barely exceed the near point resolution of the human eye. The foam may therefore be referred to as microcellular. Specimens were prepared by initial rough cutting followed by abrasive machining using abrasive paper.
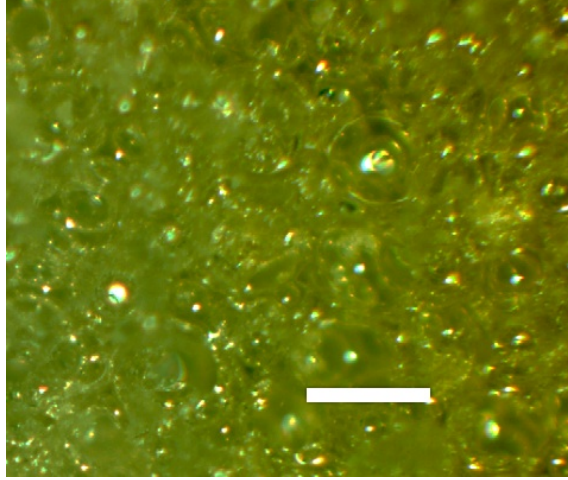
Figure 1: Dense polyurethane foam, optical image. Scale mark, 0.25 mm.

2.2 Size effects and interpretation

Size effect studies were done using broadband viscoelastic spectroscopy (BVS). Briefly (for more details, see [16]), the method makes use of a Helmholtz coil to apply torque to a magnet fixed to the specimen. Angular deformation is measured via a laser beam reflected from a small mirror attached to the specimen, upon a position sensitive silicon detector. Torque is inferred from the current in the coil. The torque channel is calibrated by tests on 6061 aluminum alloy which has well known properties. Both torsion and bending measurements can be done on the same specimen without any friction. All tests were done at a frequency 1 Hz; the frequency range of the instrument is from micro-Hertz to 100 kHz.

Size effects for round specimens in torsion were interpreted using the following exact solution [4] for a Cosserat elastic circular rod of radius r. The size effects are expressed as Ω, the ratio of structural rigidity to its classical counterpart:

$$\Omega = (1 + 6\{\frac{\ell_t}{r}\}^2)\left[\frac{1 - \frac{4}{3}\Psi\chi}{1 - \Psi\chi}\right] \tag{11}$$

Here $\chi = I_1(pr)/prI_0(pr)$, $p^2 = 2\kappa/(\alpha + \beta + \gamma)$ and I_0 and I_1 are modified Bessel functions of the first kind; ℓ_t is the characteristic length in torsion; N is the coupling number. The torsional rigidity in classical elasticity is $\frac{M}{\theta} = G[\frac{\pi}{2}r^4]$. G is the true shear modulus in the absence of gradients, M is the applied moment and θ is the angular displacement per length.

Elastic constants G, ℓ_t, Ψ and N were found by fitting Equation 11 to the full set of experimental data using MATLAB.

Size effects for square specimens in torsion were interpreted using the full solution given in [7] which is too lengthy to reproduce here. A simpler approximation for small N was tried

$$\Omega = \left[1 + \frac{21\bar{\alpha}\bar{\kappa}(89\bar{\ell}^2 + \frac{363}{898}\bar{\ell}_b^2)}{266\bar{\alpha}\bar{\kappa} + 2\bar{\ell}^2[3255\bar{\alpha}(\bar{\kappa} + 2) + 4259\bar{\kappa}] + 33\bar{\ell}_b^2[945\bar{\alpha}(1 + \bar{\kappa}/2) + 499\bar{\kappa}]}\right]. \tag{12}$$

with $\bar{\ell} = \frac{\ell_t}{a}$; $\bar{\ell}_b = \frac{\ell_b}{a}$; $\bar{\kappa} = \frac{\kappa}{G}$; $\bar{\alpha} = \frac{\alpha}{a^2 G}$ and a as the bar half width. Inferred elastic constants were similar to those from the full solution, but the full solution was superior in that the fitting was better.

Bending of round sections was interpreted via an exact expression [5] for a Cosserat elastic circular rod of radius r:

$$\Omega = 1 + 8(\frac{\ell_b}{r})^2\frac{(1 - (\frac{\beta}{\gamma})^2)}{(1 + \nu)} + \frac{8N^2}{(1 + \nu)}\left[\frac{(\frac{\beta}{\gamma} + \nu)^2}{\zeta(\delta r) + 8N^2(1 - \nu)}\right] \tag{13}$$

4

Here $\delta = N/\ell_b$ and $\zeta(\delta r) = (\delta r)^2[((\delta r)I_0((\delta r)) - I_1((\delta r)))/((\delta r)I_0(\delta r) - 2I_1(\delta r))]$. The Young's modulus E and Poisson's ratio ν were determined from compression testing. Constants ℓ_b, β/γ, and N were determined from fitting the experimental results with Equation 13. The corresponding rigidity in classical elasticity is $\frac{M}{\theta} = E[\frac{\pi}{4}r^4]$.

2.3 Warp, rotation and interpretation

Warp of the cross sections in a square section bar is of interest because warp [7] depends on ℓ_t and N but in contrast to size effects, is not very sensitive to Ψ. Also, warp entails a concentration of strain; concentrations of stress and strain including those around holes are reduced in a Cosserat solid [8]. Such concentrations of strain are of practical interest because they render the material more vulnerable to fracture where the strain is highest.

The torsion deformation field is $u_x = -\theta zy, u_y = \theta zx$, where θ is the twist angle per unit length. The warp of a classical solid is given by a double Fourier series [23] but can be well approximated [7] by $\frac{u_z(x,y)}{\theta a^2/16} = 5(x^3y - xy^3) + \frac{33}{38}(x^5y - xy^5)$ in which $2a$ is the bar width. For a Cosserat solid with $\kappa \to \infty$, corresponding to coupling number $N = 1$, the full warping displacement expression reduces to the following [7], in which $\bar{\ell} = \frac{\ell_t}{a}$ and $\bar{\ell}_b = \frac{\ell_b}{a}$ with $2a$ as the bar width:

$$\frac{u_z(x,y)}{\theta a^2/16} = \frac{10\left(38 + 2211\bar{\ell}^2 + 2772\bar{\ell}_b^2\right)(x^3y - xy^3) + 33\left(2 - 315\bar{\ell}^2\right)(x^5y - xy^5)}{4\left(19 + 465\bar{\ell}^2 + 990\bar{\ell}^4\right) + 742.5\left(6 + 49\bar{\ell}^2\right)\bar{\ell}_b^2}. \tag{14}$$

Cosserat effects result in a reduction of the warp below classical values. There is more reduction as ℓ_t increases; ℓ_b has a modest effect on the curve shape. As N is decreased from 1, warp increases proportionally until the classical value is reached for $N = 0$. Consequently if N is small the warp is predicted to differ little from the classical curve.

In the present study, warp was inferred from rotation. Warp can be measured directly via optical methods such as image analysis or holographic interferometry, however in view of the small thickness of the specimen and the smallness of displacement due to warp compared with displacement due to twist, the rotation approach was considered expedient. Two rotation stages (Newport type 472) with resolution $0.02°$ were mounted on an optical table and the specimen was cemented at each end to the center points of each stage. A specimen, 8 mm square cross section and 100 mm long was aligned horizontally and cemented between the stage centers. Small mirrors 6 mm square were cemented via slender stalks at several locations on the specimen lateral surface to measure rotation. The rotation about the x axis is

$$r_1 = \frac{1}{2}(e_{123}u_{3,2} + e_{132}u_{2,3}) \tag{15}$$

with u as displacement and e as the permutation symbol.

The rotation about the z axis is

$$r_3 = \frac{1}{2}(e_{312}u_{2,1} + e_{321}u_{1,2}). \tag{16}$$

Substituting the displacement field in Equation 15,

$$r_1 = \frac{1}{2}\left(\frac{\partial u_z}{\partial y} - \theta x\right) \tag{17}$$

The first term in r_1 represents the slope of the warp curve and the second term is due to the twist. The twist rotation is $r_3 = \theta z$ with z as the distance from the fixed end. The ratio of rotations $\frac{r_1}{r_3} = f\frac{a}{z}$ is equal to the ratio of deflection distances of the laser beam. At the specimen edge, $f = 0.92$; at the center of the top surface, 0.37 if it is classically elastic.

As for prediction of warp and rotation effects based on elastic constants from size effects, if ℓ_t / width = 1/8 corresponding to $\ell_t = 1$ mm, and if $N = 1$ then the slope of the warp curve is 0.56 of the classical value at the specimen edge, and 0.69 of the classical value at the center of the lateral surface. Because the rotation also has a contribution from the twist, the corresponding ratios of rotation, Cosserat to classical are 0.78 at the edge and 1.17 at the center. If, however, $N = 0.2$, then the rotation changes only about 4% from

5

classical; for $N = 0.1$, only 2% different. So the size effect measurements that imply a small N, predict the rotation to be very close to the classical value despite the large characteristic length.

To measure two components of rotation, a laser beam was diverged and focused, then reflected from the mirror on the specimen and projected upon a screen or upon a position sensitive silicon detector. The bar was subject to torsion by rotating the stages in opposite directions. Correction for bending due to imperfect alignment was done by rotating both stages in the same direction to achieve rotation without twist, and measuring the rotation. In further experiments intended to eliminate the need for such correction, tests were done in which one end of the specimen was coupled to the rotation stage by a layer of rubber 6 mm thick, then one stage was rotated. Error estimates were based on uncertainty in orthogonality and alignment and on variance of results from multiple experiments.

2.4   Ultrasound

Ultrasonic studies were conducted to explore anisotropy. A block of foam 22.2 by 22.8 by 65.2 mm was subjected to tone burst waveforms input from a signal generator (Tektronix AFG 3051C) to a broadband transducer (Panametrics V102 longitudinal; V153 shear) of natural frequency 1 MHz. A similar transducer was used to detect the waves; the signal was input to a digital oscilloscope (Tektronix DPO 3014). Longitudinal and shear waves at frequencies from 1 MHz to 0.3 MHz were used. Wave velocities were calculated from pulse travel time and specimen thickness. Moduli were inferred from the velocity and density.

3   Results

3.1   Size effects

Size effects in torsion of a square cross section bar are shown in Figure 2. The rigidity ratio Ω is the ratio of observed structural rigidity to the asymptotic value for large thickness in which gradients tend to zero. Observed size effects are modest in magnitude compared with effects found in low density open cell foams and in lattices and are similar to those found in round specimens of dense foam. Inferred elastic constants were found to be

$$G = 109 MPa, \ell_t = 1.08mm, N = 0.12, \Psi = 1.49856 \tag{18}$$

The goodness of fit was $R^2 = 0.999977$. Torsional size effects for square section bars have minimal dependence [7] on ℓ_b; a value of 0.327 mm was input. It is not surprising that the modulus differs somewhat from that of the round specimen series because the batch of material, albeit of similar density, was different.
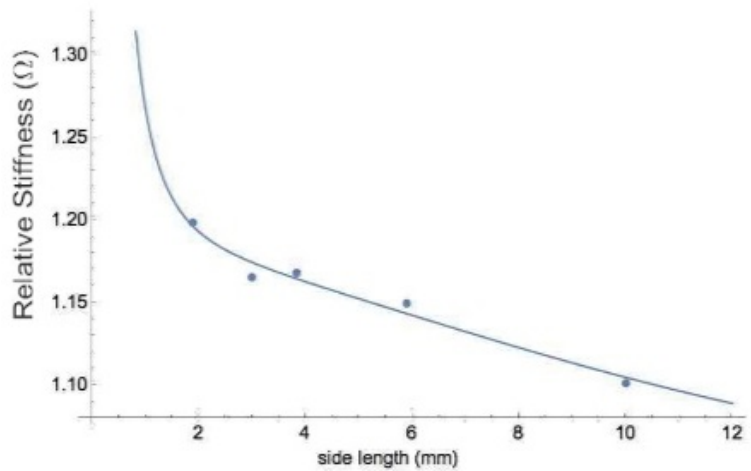
Figure 2: Size effects in torsion of a square cross section bar. Rigidity ratio Ω vs. width. Points are experimental. Curve fit is based on the full solution for a square section. For a classical solid, $\Omega = 1$ independent of diameter.

The inferred value of ℓ_t is larger than was found earlier for the round case and N is smaller, therefore the original torsion data for round sections were re-plotted and refitted using MATLAB. Results assuming $\Psi = 1.5$ and $\ell_t = 0.6$ mm are shown in Figure 3. The fit resulted in $G = 104$ MPa and $N = 0.196$, almost identical to the original value 0.2. The goodness of fit was $R^2 = 0.94$. The original curve fits were done to achieve a consistent set of constants for both torsion and bending. Because of limitations in available software the original fits were done assuming Ψ at widely spaced discrete values. The elastic constants inferred assuming $\Psi = 1.5$ are similar to the ones obtained originally.
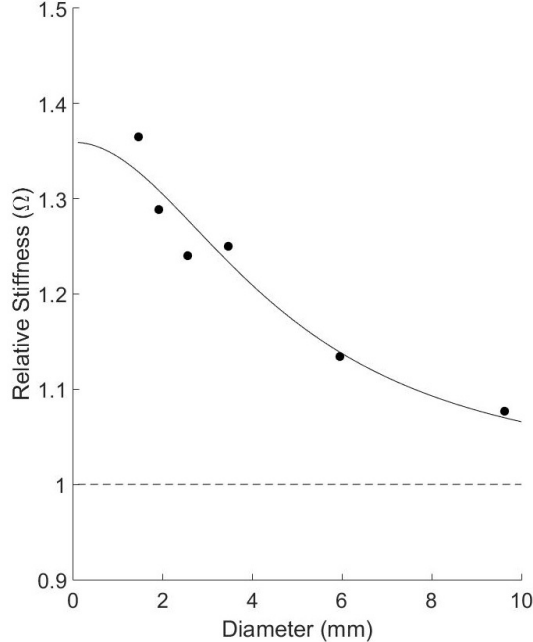
Figure 3: Size effects in torsion of a round cross section bar. Rigidity ratio Ω vs. diameter. Points are experimental. Curve fit is based on the exact solution for round section assuming $\Psi = 1.5$. For a classical solid, $\Omega = 1$ independent of diameter as indicated by the horizontal dashed line.

Further analyses of round specimen size effects were done allowing Ψ to vary in fine increments of 0.001. A value of Ψ slightly smaller than 1.5 resulted in inferred values from round section data much closer to those found in the present study for square sections (Figure 2) as shown in Figure 4. The corresponding elastic constants are

$$G = 104 MPa, \ell_t = 0.9mm, N = 0.152, \Psi = 1.493 \tag{19}$$

The goodness of fit was $R^2 = 0.949$, slightly higher than that for $\Psi = 1.5$. Because the curve shape depends on several parameters, a range of values allows fitting with similar quality. Results for round and square sections indicate $\ell_t \approx 1$ mm, Ψ approaching but below its upper limit 1.5, and N small, from 0.12 to 0.15; with modest quantitative differences. If, however, one assumes the constants found from the square section (with N free) as input to a fit for the round section data, then $N = 0.144$ and $R^2 = 0.65$. The difference between the round section and square section specimens is therefore likely real, for the following reasons.

Foams differ from lattices in that foams have a surface layer of incomplete cells. There may also be surface damage due to the machining process. Such damage reduces the rigidity of specimens, especially small ones, so it reduces the inferred characteristic length below the actual value. The damage may differ depending on preparation method. Some of the difference between round and square specimens is attributed to such phenomena.

For foams [22], neglecting effects of air in the cells, as is appropriate for a stiff foam, the foam Young's modulus E is

$$\frac{E}{E_s} = C_f [\frac{\rho}{\rho_s}]^2, \tag{20}$$

in which ρ_s is the density, C_f is a constant of value near one, and E_s is the modulus of the solid material of which the foam is made. Assuming for stiff polymer a solid density of 1100 kg/m^3 and $C_f = 1$, then given the density of the present foam, if $E = 300$ MPa, the value actually originally inferred for the asymptotic modulus, then the solid phase $E_s = 3.14$ GPa, which is reasonable for a glassy polymer. This foam is too dense for its structure to be viewed as an assemblage of ribs or plates in bending; even so, the quadratic

8

dependence on density is experimentally observed even as the density approaches that of the solid material [22]. Therefore the Young's modulus of the present foam is reasonable in the view of the known behavior of similar materials.
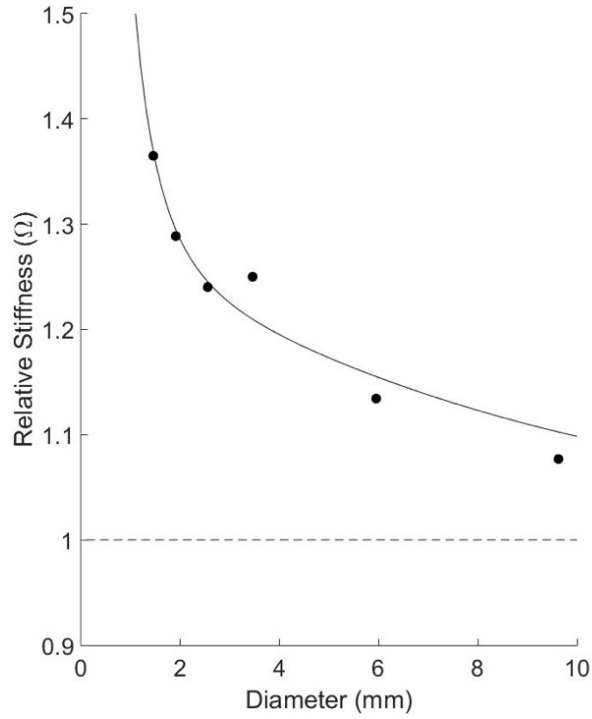

Figure 4: Size effects in torsion of a round cross section bar. Rigidity ratio Ω vs. diameter. Points are experimental. Curve fit is based on the exact solution for round section with Ψ allowed to freely vary. For a classical solid, $\Omega = 1$ independent of diameter as indicated by the horizontal dashed line.
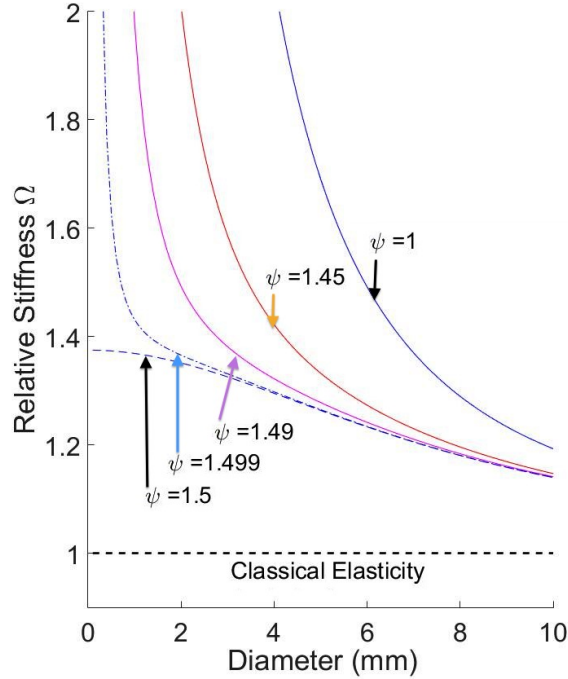
Figure 5: Size effects; theoretical dependence of torsion rigidity ratio Ω vs. diameter upon Ψ for $N = 0.2$ and $\ell_t = 1$ mm. From top down, $\Psi = 1.0, 1.45, 1.49, 1.499, 1.5$. For a classical solid, $\ell_t = 0$ so $\Omega = 1$ independent of diameter as indicated by the horizontal dashed line.

Observe (Figure 3) that Ψ at its upper limit 1.5 gives rise to an intercept of the curve vs. diameter to a finite value of the rigidity ratio Ω. If $\Psi < 1.5$ then the curve tends to infinity near the origin; as $\Psi \to 1.5$, the asymptotic rise becomes closer to the origin (Figure 5). Such a singularity need not present problems experimentally because in real materials one cannot prepare meaningful specimens smaller than the smallest microstructure.

As for other generalized continuum theories, if one forces $N = 1$ as in couple stress elasticity, the fit is poor with $R^2 = 0.003$. Modified couple stress theory requires $\frac{\beta}{\gamma} = 1$ in addition to $N = 1$, so that will fit poorly as well. If one forces a classical elastic interpretation with $\ell_t = 0$, then $R^2 = -5.1$. Therefore for this material, Cosserat elasticity is a superior representation compared with couple stress elasticity (including its restricted form) or classical elasticity.

Specific comparison of the magnitude of effects with other materials is as follows. As for size effects, the maximum Ω was about a factor 6.5 in low density open cell polymer foam [14], a factor 12 in negative Poisson's ratio foam [15] and a factor 36 in a designed lattice [16] compared with less than a factor of 1.4 in the present dense foam. The difference is associated with the small value of N in the dense foam compared with large values, 1 or approaching 1, in the open cell foams and lattices. A composite with stiff spherical inclusions was found to have exhibit no size effects, hence a characteristic length of zero [4]. Homogenization analysis of composites containing stiff spheres disclosed characteristic lengths of zero [21]. In homogenization analysis of 2-D chiral honeycomb lattices with slender ribs, the Cosserat characteristic lengths are comparable to the cell size [18] and N approaches its upper limit of 1.

3.2 Warp and rotation

Warp is expected to be nearly classical if N is small. Size effect measurements indicate Cosserat elastic behavior with weak coupling, $N = 0.12$ to 0.15. For such N, the predicted warp does not differ much from classical values. Warp inferred from measured rotation is via Equation 17. Figure 6 shows normalized warp

$W = \frac{u_z(x,y)}{\theta a^2/16}$ predicted by classical elasticity and warp predicted by Cosserat elasticity with $N = 1$ and with $\ell_t = 2a/8$. The warp inferred from experimental rotation was nearly classical as shown in the figure. Specifically, at the edge of the surface, the rotation r_1 was 96% $\pm$ 3% of classical compared with 97% of classical for $N = 0.15$ and 78% of classical for $N = 1$. At the center of the surface, the rotation r_1 was 103% $\pm$ 3% of classical compared with 103% of classical for $N = 0.15$ and 117% of classical for $N = 1$. The measurements indicate, assuming a deviation twice the error estimate, $N < 0.3$. The inference of warp from rotation is therefore consistent with a small value of N but not with $N = 1$. To accurately measure such small values of N from rotation, considerable improvement in accuracy and precision of the rotation measurement would be required.
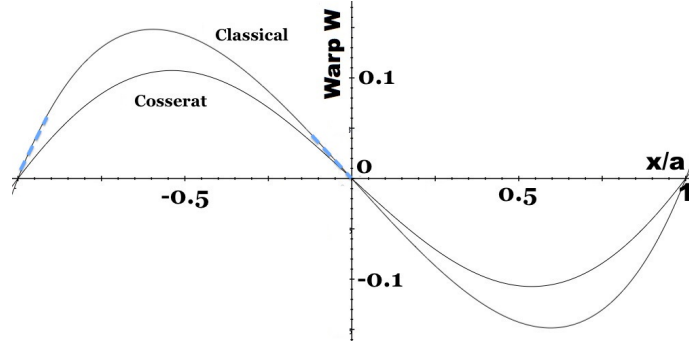

Figure 6: Normalized warp W vs. normalized position on the surface of a classical solid and of a Cosserat solid with $N = 1$ and with $\ell_t =$ width / 8. Experimental slopes are shown by thick blue dash lines.

3.3 Ultrasonic waves

Ultrasonic measurements revealed a slight anisotropy. Comparisons of torsion and bending behavior based on Eq. 11 and Eq. 13 are fully applicable only in isotropic materials. Foams, especially compliant foams of low density, are not necessarily isotropic because during fabrication the cells are formed from expansion of bubbles under gravity and under partial constraint by mold. Elastic properties of lattices are governed by their structural symmetry; they are not in general isotropic. For the present foams, ultrasonic measurements revealed tensorial moduli, in the reduced notation, $C_{11} = 531$ MPa, $C_{22} = 557$ MPa, $C_{33} = 574$ MPa based on longitudinal waves and shear moduli $G_1 = 143$ MPa, $G_2 = 151$ MPa, $G_3 = 146$ MPa based on shear waves. The maximum anisotropy ratio was 1.08 for the C modulus and 1.06 for the shear modulus. Moduli are higher at 1 MHz than those obtained at 1 Hz as is expected in a polymeric viscoelastic material. Damping calculated from viscoelastic dispersion of a factor 1.38 in shear modulus over a factor 10^6 in frequency is tan $\delta = 0.037$, which is reasonable for the polymer solid phase. The Poisson's ratio obtained from averages of longitudinal v_L and shear wave v_s speeds was $\nu = 0.32$ via the following

$$\nu = \frac{1 - 2(v_s/v_L)^2}{2 - 2(v_s/v_L)^2} \tag{21}$$

Such a Poisson's ratio is reasonable for this sort of foam [22].

As for the interpretation of C_{1111} (C_{11} in the reduced notation) for isotropic elastic materials in relation to Young's modulus E, [23]

$$C_{1111} = E\frac{1 - \nu}{(1 + \nu)(1 - 2\nu)} \tag{22}$$

So, at 1 MHz, $E = 387$ MPa; the ratio with respect to the value at 1 Hz is a factor 1.29, somewhat less than the ratio for shear; such a difference in viscoelastic dispersion is reasonable.

The slight anisotropy revealed by ultrasonic measurements is pertinent to the use of torsion and bending results to obtain elastic constants, both in classical elasticity and in Cosserat elasticity. Using the Poisson's ratio $\nu = 0.32$ derived from ultrasound and relaxing the isotropic requirement $E = 2G(1 + \nu)$ (by 9% in view

11

of ultrasonic results), the bending data for a circular section yield the following elastic constants, assuming $N = 0.152$ from torsion (Eq. 19) and invoking for consistency $\frac{\ell_t^2}{\ell_b^2} = 2(\frac{\beta}{\gamma} + 1)$ based on the definition of ℓ_t and ℓ_b,
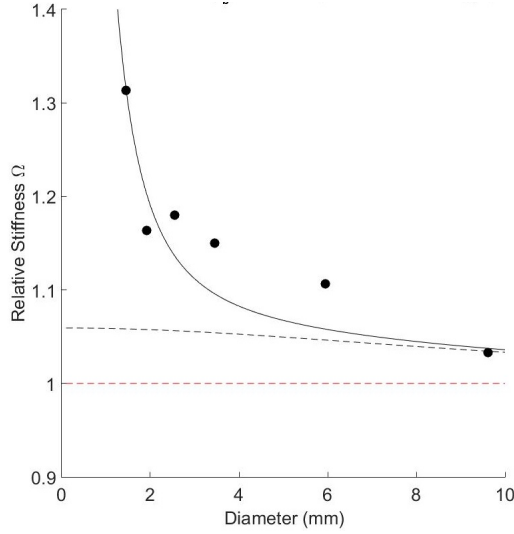

Figure 7: Size effects in bending of a round cross section bar. Rigidity ratio Ω vs. diameter. Points are experimental. Curve fit (solid curve) is based on the exact solution for round section with $\frac{\beta}{\gamma}$ allowed to freely vary. Dashed curve is for $\frac{\beta}{\gamma} = 1$. For a classical solid, $\Omega = 1$ independent of diameter as indicated by the horizontal dashed line.

$$E = 300 MPa, \ell_b = 0.456 mm, N = 0.152, \frac{\beta}{\gamma} = 0.944 \tag{23}$$

The goodness of fit was $R^2 = 0.79$. If one attempts to force $\frac{\beta}{\gamma} = 1$ then $R^2 = -1.43$, a poor fit because such an assumption gives rise to an intercept of small magnitude on the ordinate as shown in Figure 7. So modified couple stress elasticity [11] is inapplicable here too because it assumes $\frac{\beta}{\gamma} = 1$ as well as $N = 1$. If one assumes only $N = 1$, allowing variation in characteristic length, then the fit yields $\ell_b = 3$ mm and predicted rigidity far too high, so a very poor fit: $R^2 = -109$. Consequently, an assumption, following [12], of limiting values of Ψ and $\frac{\beta}{\gamma}$ is inconsistent with torsion and bending results respectively for this material.

Ultrasonic studies reveal more than moduli derived from wave velocity. There was minimal distortion of the tone burst but the transmitted signal was weak. Signal strength increased as frequency was lowered from 1 MHz. There was no obvious dependence of signal velocity upon frequency (dispersion) in the range 0.3 to 1 MHz. Shear waves were difficult to discern above 0.5 MHz. Cut-off frequencies associated with resonance of structural elements are known to occur in heterogeneous materials. Heterogeneous materials with random structure differ from those with a periodic structure. For example, in a random particulate composite [35] of 0.15 mm diameter glass spheres in epoxy, wave propagation was found to be fairly non-dispersive; only when the wavelength became equal to the inclusion radius did the tone burst become sufficiently distorted to prevent velocity measurements. Longitudinal waves were propagated up to about 5 MHz; attenuation increased with frequency to a much greater extent than in the matrix alone. In a layered composite [36] containing periodic arrays of spheres, pass bands and stop bands were observed at ultrasonic frequencies. Furthermore, tungsten wires 0.127 mm in diameter spaced 0.3 mm apart in aluminum alloy, the stop band begins at about 5.5 MHz [26]. As for a possible generalized continuum interpretation, Cosserat elasticity does predict dispersion of shear waves; micromorphic / microstructure elasticity predicts dispersion of longitudinal waves as well as cut off frequencies. Such interpretation is not pursued here because in a viscoelastic material wave dispersion is also associated with damping: a confounding variable. In the dense foam, viscoelastic loss may suffice to account for the apparent cut off of wave propagation at high frequencies.

3.4 Generalized continuum theories: comparison

Cosserat elasticity and theories with less freedom have been explored in the interpretation of quasi-static phenomena in a dense foam. Classical elasticity does not apply to this material because it does not capture the size effects observed. An assumption of couple stress elasticity [9], corresponding to $N = 1$ in the Cosserat interpretation, does not apply because it gives rise to very poor fits of the size effect results in both torsion and bending. Moreover, the inferred warp of a square section bar is consistent with a small N, not $N = 1$. Modified couple stress theory [11] requires $\frac{\beta}{\gamma} = 1$ as well as $N = 1$; this also gives poor fits to size effect results. If one assumes only $\frac{\beta}{\gamma} = 1$, and allows N free, the fit is also poor. Restricted Cosserat elasticity [12] does not apply either, because its assumption of $\Psi = 1.5$ fails to fit the size effects in torsion and its assumption of $\frac{\beta}{\gamma} = 1$ fails to fit the size effects in bending. The goal of eliminating the predicted divergence of rigidity has merits but if experimental results call for a restricted range of parameters, that will show up in the curve fits. While some assumptions may simplify the mathematics, that is not the case for $\frac{\beta}{\gamma} = 1$; for bending, the solution for both round and square cross sections is simplified for $\frac{\beta}{\gamma} = -\nu$. In any case, the restricted models do not apply to the present dense foam. As for other studies pertinent to N, planar model materials made by machining an array of circular holes into aluminum bars [19] were studied for size effects and were interpreted via Cosserat elasticity. The holes were 3.5 mm in diameter and were spaced 12.7 mm and 16 mm in different directions. Parameters obtained were $E = 39$ GPa, $\ell_b = 10.14$ mm, $N = 0.112$; the effect of N was modest over the range considered.

The set of dense foam Cosserat elastic constants in Eq. 19 (torsion) and Eq. 23 (bending) is consistent with the exception of a relaxation of the isotropic requirement $E = 2G(1 + \nu)$ by 9% based on a slight anisotropy revealed by the ultrasonic results. Values differ somewhat from those obtained from square specimens (Eq. 18). The difference is attributed mostly to differences in incomplete cells and surface damage associated with specimen preparation. The inference of small N in dense foam is robust to such variations.

Suggestions to restrict ranges of elastic constants are not new. In the early development of the theory of elasticity, it was proposed that Poisson's ratio is 1/4 for all isotropic materials based on a specific model, due to Navier, assuming central forces between atoms [24] [25]. Experiments revealed a range of Poisson's ratio, showing the model to be overly restrictive.

As for generalized continuum theories with freedom similar to that of Cosserat elasticity, the theory of elasticity with voids [27] provides sensitivity to dilatation gradient but has no rotational degrees of freedom; there are a total of 5 isotropic elastic constants. The theory of voids [27] when considered alone, gives rise to size effects in bending but not in torsion so it does not apply to the present dense foam. Micro-strain elasticity allows sensitivity to gradients of local strain. A homogenization analysis [28] based on micro-strain elasticity was applied to porous media. This theory incorporates two nonclassical parameters corresponding to the diameter and spacing of pores and two parameters based on the elastic moduli of the solid matrix. The theory predicts size effects [29] similar to those of Cosserat elasticity. The displacement field in the bending analysis is identical to the classical field. That prediction differs from that of Cosserat elasticity in which square section bars undergo sigmoid deformation of the lateral surfaces [6]. Warp in torsion was not considered in the micro-strain analysis. The micro-strain theory predicts size effects in torsion and bending to be of the same magnitude; it worked well to interpret [29] size effects in a low density polymethacrylamide foam [30]. For that foam a Cosserat interpretation based on approximate solutions for square cross section gave bending and torsion characteristic lengths of similar magnitude, $\ell_t \approx \ell_b$. Strictly, a purely Cosserat solid obeys $\frac{\ell_t^2}{\ell_b^2} = 2(\frac{\beta}{\gamma} + 1)$ (Eq. 10) from the definitions of the lengths; because $|\frac{\beta}{\gamma}| < 1$ based on stability conditions, $\ell_t < 2\ell_b$. So the low density foam is likely to have sensitivity to other gradients in addition to those of rotation, perhaps those associated with the microstrain concept. Holographic study of dense foam [31] disclosed nonclassical strain at the corner of a square section bar in torsion; such deformation can be understood within Cosserat elasticity. Because micro-strain elasticity requires the Cauchy stress to be symmetric, such corner deformation will not appear in that theory.

There are also theories with more freedom than Cosserat elasticity. Microstretch elasticity [32] incorporates the freedom of Cosserat elasticity as well as sensitivity to gradient of local dilatation; there are 9 isotropic elastic constants. Microstretch elasticity is a subset of microstructure / micromorphic elasticity [33] [34] which allows 18 isotropic elastic constants. The torsion results considered here are insensitive to

dilatation gradient effects even they are present. For the present dense foam, dilatation gradient effects, if present, are likely to be small because such effects would give rise to an effective bending characteristic length too large to be subsumed within a Cosserat representation. By contrast, in the dense foam, a consistent set of elastic constants for bending and torsion (with the exception of a slight anisotropy of modulus revealed by ultrasound) was obtained assuming Cosserat elasticity.

3.5 Summary and implications

Results are consistent with a Cosserat interpretation in which the elastic constants are not at their extreme limits. In particular, couple stress theory and its variants are not consistent with the results. Effects of dilatation gradient appear to be too small to be discerned in the dense foam. It is possible that a microstrain model may apply to the observed size effects but not to nonclassical deformation of bars of square cross section.

Implications for future experiments are as follows. It is desirable to have as wide a range as possible of specimen width values. For example, even though the cells are smaller than 0.2 mm and the largest cells are barely visible on visual inspection, specimens 10 mm thick do not suffice for the asymptotic moduli to be approached. Thicker specimens would provide a more definitive value of the asymptotic moduli and tighter constraints on the remaining constants. Similarly, thinner specimens would provide improved values for Ψ and N. As for other generalized continuum theories, to interpret experiments, one must have solutions of the appropriate boundary value problems.

4 Conclusions

A dense polyurethane foam exhibits size effects with a characteristic length considerably larger, by more than a factor of 6, than the cell size. The Cosserat coupling number N is shown to be small via several methods. Assumption of limiting values of N, Ψ or $\frac{\beta}{\gamma}$ as suggested by several authors is shown to be inapplicable to this dense foam. Comparison of square and round sections suggests a modest effect of incomplete cells or damage at the surface in reducing the apparent characteristic length. A consistent set of elastic constants for bending and torsion (with the exception of a slight anisotropy of modulus revealed by ultrasound) was obtained assuming Cosserat elasticity. This suggests a minimal role for dilatation gradients associated with void / microstretch theory in this material.

5 Acknowledgments

References

[1] Cosserat, E. and Cosserat, F. *Theorie des Corps Deformables*, Hermann et Fils, Paris (1909).

[2] Mindlin, R. D., Stress functions for a Cosserat continuum, Int. J. Solids Structures, **1**, 265-271 (1965).

[3] Eringen, A. C. Theory of micropolar elasticity. In Fracture Vol. **1**, 621-729 (edited by H. Liebowitz), Academic Press, New York (1968).

[4] Gauthier, R. D. and W. E. Jahsman, A quest for micropolar elastic constants. J. Applied Mechanics, **42**, 369-374 (1975).

[5] Krishna Reddy, G. V. and Venkatasubramanian, N. K., On the flexural rigidity of a micropolar elastic circular cylinder, J. Applied Mechanics **45**, 429-431 (1978)

[6] Lakes, R. S. and Drugan, W. J., Bending of a Cosserat elastic bar of square cross section - theory and experiment, Journal of Applied Mechanics, **82**(9), 091002 (8 pages) (2015)

[7] Drugan, W. J. and Lakes, R. S., Torsion of a Cosserat elastic bar with square cross section: theory and experiment, Zeitschrift fur angewandte Mathematik und Physik (ZAMP), **69** (2), 24 pages (2018).

[8] Mindlin, R. D., Effect of couple stresses on stress concentrations, Experimental Mechanics, **3**, 1-7, (1963)

[9] Koiter, W. T., Couple-Stresses in the theory of elasticity, Parts I and II, Proc. Koninklijke Ned. Akad. Wetenshappen **67**, 17-44 (1964).

[10] Hadjesfandiari, A. R. and Dargush, G. F., Couple stress theory for solids, Int. J. Solids Structures **48**, 2496-2510 (2011).

[11] Yang, F. Chong, A.C.M. Lam, D.C.C. Tong, P. Couple stress based strain gradient theory for elasticity, International Journal of Solids and Structures 39 2731-2743 (2002)

[12] Neff, P Jeong, J Fischle, A Stable identification of linear isotropic Cosserat parameters: bounded stiffness in bending and torsion implies conformal invariance of curvature, Acta Mechanica 211, (3-4), 237-249 (2010)

[13] Lakes, R. S., Experimental microelasticity of two porous solids, International Journal of Solids and Structures, 22 55-63 (1986).

[14] Rueger, Z. and R. S. Lakes, Experimental Cosserat elasticity in open cell polymer foam, Philosophical Magazine, **96**, 93-111 (2016).

[15] Rueger, Z. and R. S. Lakes, Cosserat elasticity of negative Poisson's ratio foam: experiment, Smart Materials and Structures, **25**, 054004, 8pp, (2016).

[16] Rueger, Z. and Lakes, R. S., Strong Cosserat elasticity in a transversely isotropic polymer lattice, Physical Review Letters, 120, 065501 Feb. (2018).

[17] A. Merkel and V. Tournat, Experimental Evidence of Rotational Elastic Waves in Granular Phononic Crystals, Phys. Rev. Lett., **107**(22), 225502 (2011).

[18] A. Spadoni and M. Ruzzene, Elasto-static micropolar behavior of a chiral auxetic lattice, J. Mechs Physics of Solids, **60**, 156-171 (2012).

[19] A.J. Beveridge, M.A. Wheel, D.H. Nash, The micropolar elastic behaviour of model macroscopically heterogeneous materials, International Journal of Solids and Structures 50 246-255 (2013)

[20] General Plastics Company, 4910 Burlington Way, Tacoma, WA 98409 https://www.generalplastics.com/

[21] D. Bigoni and W. J. Drugan, Analytical derivation of Cosserat moduli via homogenization of heterogeneous elastic materials, J. Appl. Mech., **74**, 741-753 (2007).

[22] Gibson, L. J. and Ashby, M. F., *Cellular Solids*, Pergamon, Oxford; 2nd Ed., Cambridge (1997).

[23] Sokolnikoff, I. S., *Theory of Elasticity*, Krieger; Malabar, FL, (1983).

[24] Weiner, J.H. 1983 *Statistical Mechanics of Elasticity*, J. Wiley, NY

[25] Timoshenko, S. P. 1983 *History of Strength of Materials*, Dover, NY

[26] D. S. Drumheller and H. J. Sutherland, A Lattice Model for Stress Wave Propagation in Composite Materials, J. Appl. Mech. 40(1): 149-154 1973

[27] Cowin, S. C. and Nunziato, J. W., Linear elastic materials with voids, J. Elasticity 13 125-147 (1983)

[28] Hütter, G., Mülich, U., and Kuna, M., Micromorphic homogenizationn of a porous medium: elastic behavior and quiasi-brittle damage, Continuum Mechanics and Thermodynamics, 27, 1059-1072, (2015).

[29] Hütter, G., Application of a microstrain continuum to size effects in bending and torsion of foams, Int. J. Engineering Science, 101, 81-91, (2016).

[30] Anderson, W. B. and Lakes, R. S., Size effects due to Cosserat elasticity and surface damage in closed-cell polymethacrylimide foam, Journal of Materials Science, 29, 6413-6419, (1994).

[31] R. S. Lakes, D. Gorman, and W. Bonfield, Holographic screening method for microelastic solids, J. Materials Science, **20**, 2882-2888 (1985).

[32] Eringen, A. C., Theory of thermo-microstretch elastic solids, Int. J. Engng. Sci., **28** (12)1291-1301, (1990).

[33] Mindlin, R. D., Micro-structure in linear elasticity, Arch. Rational Mech. Analy, **16**, 51-78, (1964).

[34] Eringen, A.C., Suhubi, E.S. Nonlinear theory of simple micro-elastic solids-I. Int. J. Engng. Sci., (2), 189-203 (1964)

[35] V. K. Kinra, A Anand, Wave propagation in a random particulate composite at long and short wavelengths, International Journal of Solids and Structures 18(5): 367-380, 1982

[36] V. K. Kinra, E. Ker, An experimental investigation of pass bands and stop bands in two periodic particulate composites, International Journal of Solids and Structures 19(5): 393-410, 1983